CHAPTER

Semiconductors

9

CHAPTER OUTLINE

9.1 INTRODUCTION

In Chapter 4 (section 4.9), we discussed that by using elementary band theory, crystalline solids can be divided into three major categories: metals, insulators, and homogeneous semiconductors. The metals are good conductors (with the exception of the divalent metals) because either the conduction band is half-filled (monovalent or trivalent metals), or there is significant overlap between the valence and conduction band (divalent metals). The crystalline solids with four valence electrons per unit cell can either be an insulator or a homogeneous semiconductor, depending on the energy gap between the valence band and the conduction band. The energy gap E_g is defined as the energy between the bottom of the lowest-filled band(s) and the top of the highest-filled bands(s). In the case of both insulators and semiconductors, the lowest unoccupied band is known as the conduction band, and the highest occupied

Physics of Condensed Matter. DOI: 10.1016/B978-0-12-384954-0.00009-8

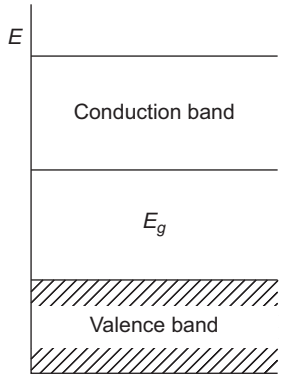

FIGURE 9.1

Schematic diagram of the valence and conduction bands.

band is known as the valence band. A schematic diagram of the valence and conduction bands, which are the energy bands in the reduced zone scheme, is shown in Figure 9.1.

At $T = 0$, the valence band is full, and the conduction band is empty for both insulators and semiconductors. Thus, the conductivity of both types of solids is zero because no carriers would be available in either of the bands to be excited by an external electric field unless the electric field (DC) is sufficiently large to cause Zener tunneling (Chapter 8) or the frequency ω of the AC electric field is such that $\hbar\omega > E_g$. At $T \neq 0$, a few electrons would be thermally excited to the conduction band, leaving behind a few positively charged holes in the valence band (as we will show, the probability of such transition is $e^{-E_g/2K_BT}$). If the energy gap is large so that very few electrons are thermally excited from the valence band to the conduction band at the room temperature, a negligible number of carriers in either of the bands would be available to conduct electricity, and essentially no current would be generated. This type of solid, which carries no current in an electric field, is known as an insulator. However, if the energy gap is small enough, a significant number of electrons are thermally excited at room temperature to the conduction band(s), leaving an equal number of positively charged "holes" at the top of the valence band(s). Thus, there are both "positively" charged carriers in the valence band and "negatively" charged carriers in the conduction band to conduct electricity and generate a perceptible current when an external field is applied. These solids are known as homogeneous semiconductors. The homogeneous semiconductors are also known as intrinsic semiconductors to distinguish them from impurity (doped) semiconductors. Thus, the distinction between the semiconductors and insulators depends essentially on the magnitude of the energy gap, and as a rule of the thumb, solids with $E_g < 2\,\text{eV}$ are semiconductors, whereas solids with $E_g > 2\,\text{eV}$ are insulators. However, most semiconductors have a much smaller energy gap.

There are two types of homogeneous semiconductors: the semiconducting elements and the semiconducting compounds. The most popular and widely used semiconducting elements are Si and Ge, both of which belong to column IV of the periodic table and crystallize in the diamond structure. The Bravais lattice of the diamond structure has a basis of two atoms, each of which has 8 *sp* electron states, but only 4 of these are occupied by electrons. The Brillouin zones have to accommodate 16 electron states, but only 8 electrons (from the two atoms) fill them. Therefore, the band structure has 8 subbands, 4 of which are completely filled and the other 4 are completely empty at 0° K. The energy gap of Si is 1.11 eV and that of Ge is 0.74 eV. These are also known as indirect semiconductors because the bottom of the conduction band does not lie directly above the top of the valence band, and thus, they have an indirect energy gap. The absorption of a photon creates an electron-hole pair, in which both the energy and momentum have to be conserved, but the momentum of a photon is negligible compared to that of the electrons. Thus, neither Si nor Ge is a good material for most optical applications because the two bands are not directly above each other. However, Si and Ge are extensively used in electronics because they can be easily doped with impurities. The other elemental semiconductors

Table 9.1 Comparison of Calculated Bandwidth with Photoemission Data for the Homopolar Materials (Energy in eV)

	Quasiparticle Theory	Expt.
Diamond	23.0	24.2 ± 1
Si	12.0	12.5 ± 0.6
Ge	12.8	12.9 ± 0.2

Reproduced from Louie[8] with the permission of Elsevier.

from column IV of the periodic table are gray tin, which has a very small energy gap (0.1 eV), red phosphorus, boron (1.5 eV), selenium, and tellurium (0.35 eV), which are solids with complex crystal structures. These semiconductors are neither used in optical applications nor in electronics. An example of the compound semiconductors of column IV of the periodic table is SiC, which has an indirect energy gap of 2.2 eV.

An example of the calculated and experimental bandwidth for the homopolar materials Si, Ge (both semiconductors), and diamond (insulator) is shown in Table 9.1.

The III–V semiconductors are crystals composed from columns III and V of the periodic table and have zincblende structure with predominantly covalent bonding. In the III–V zincblende semiconductors such as GaAs and InSb, Ga and In have three outer electrons, whereas As and Sb have five outer electrons. Ga or In occupies all the A sites in the diamond structure, whereas As or Sb occupies all the B sites (see Figure 6.4 in Chapter 6). The most popular of these is GaAs, which has a direct energy gap of 1.43 eV and thus facilitates the absorption of photons creating electron-hole pairs. GaAs is therefore widely used in optical applications. InSb has a direct energy gap of 0.18 eV. The other III–V semiconductors are GaN, GaSb, InP, and InAs, which have direct energy gaps of 3.44 eV, 0.7 eV, 1.34 eV, and 0.36 eV, respectively.

The essential features of the band structure of Ge are shown in Figure 9.2. In Ge, which

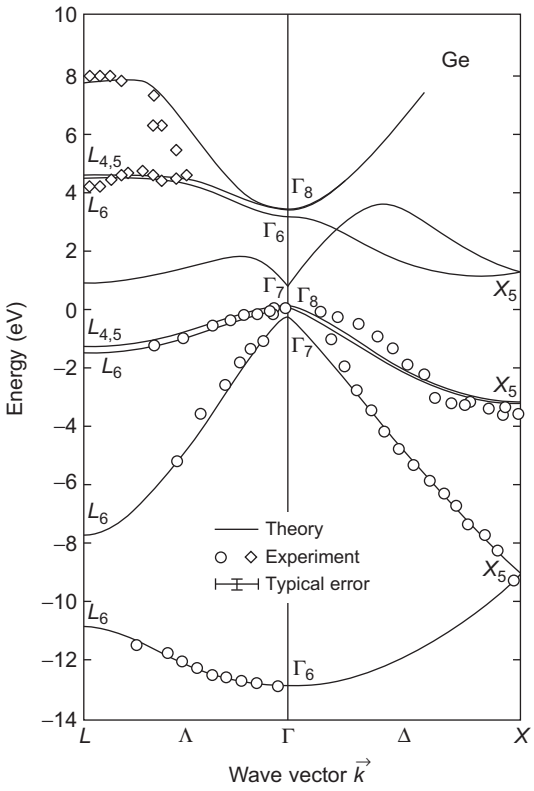

FIGURE 9.2

Calculated quasiparticle energies of Ge versus direct (○) and inverse (◇) photoemission data.

Reproduced from Louie[8] with permission of Elsevier.

has an indirect energy gap, the top of the valence band is at Γ, but the bottom of the conduction band is at *L*. In contrast, GaAs (not shown in the figure), which has a direct energy gap, both the top of the valence band and the bottom of the conduction band are at Γ.

9.2 ELECTRONS AND HOLES

In an intrinsic semiconductor at room temperature, the carriers are the electrons excited to the bottom of the conduction band from the top of the valence band. Because the filled valence band has no net charge (there are as many electrons as positively charged ions), the absence of an electron creates a net positive charge in the band. In addition, we consider the effective inverse mass tensor of an electron introduced in Eq. (8.35):

$$[\mathbf{M}_n^{-1}(\mathbf{k})]_{ij} = \frac{1}{\hbar^2}\frac{\partial^2 \varepsilon_n}{\partial k_i \partial k_j}. \tag{9.1}$$

We also derived an expression for the mass tensor in Eq. (8.37) by using perturbation theory,

$$[\mathbf{M}_n^{-1}(\mathbf{k})]_{ij} = \frac{1}{m}\delta_{ij} + \frac{\hbar^2}{m^2}\sum_{n' \neq n}\frac{<n\mathbf{k}|-i\nabla_i|n'\mathbf{k}><n'\mathbf{k}|-i\nabla_j|n\mathbf{k}> + c.c.}{\varepsilon_n(\mathbf{k}) - \varepsilon_{n'}(\mathbf{k})}. \tag{9.2}$$

At the top of the valence band, the inverse effective mass tensor can either be positive or negative. Because the concept of a negative mass is contrary to our physical understanding, the empty state at the top of the valence band can be considered as a positively charged "hole" with a positive effective mass. This concept of the positively charged holes is very important in formulating a theory for the semiconductors. We introduce the general definition of the effective mass tensor for both electrons and holes,

$$[\mathbf{M}_n^{-1}(\mathbf{k})]_{ij} = \pm\frac{1}{\hbar^2}\frac{\partial^2 \varepsilon_n}{\partial k_i \partial k_j}, \tag{9.3}$$

where the positive sign is for electrons and the negative sign is for holes. Because the bottom of the conduction band is at ε_c and the top of the valence band is at ε_v, we can express the energy of the electrons $(\varepsilon_e(\mathbf{k}))$ and holes $(\varepsilon_h(\mathbf{k}))$ as

$$\varepsilon_e(\mathbf{k}) = \varepsilon_c + \frac{\hbar^2}{2}\sum_{ij} k_i (\mathbf{M}_e^{-1})_{ij} k_j \tag{9.4}$$

and

$$\varepsilon_h(\mathbf{k}) = \varepsilon_v - \frac{\hbar^2}{2}\sum_{ij} k_i (\mathbf{M}_h^{-1})_{ij} k_j. \tag{9.5}$$

However, there are two types of effective hole masses (light holes and heavy holes) for Si, Ge, and GaAs. At the valence band maximum, there are two degenerate bands at Γ, while the third band (there are three degenerate bands in the absence of spin) is lowered due to spin-orbit interaction. The band

with the low curvature results in holes with large effective mass (heavy holes), whereas the band with the high curvature has holes with small effective mass (light holes), which is evident from Eq. (9.3).

One can write the effective mass tensor in terms of a set of orthogonal principal axes,

$$\varepsilon_e(\mathbf{k}) = \varepsilon_c + \frac{\hbar^2}{2}\sum_i (\mathbf{M}_e^{-1})_{ii} k_i^2 \tag{9.6}$$

and

$$\varepsilon_h(\mathbf{k}) = \varepsilon_v - \frac{\hbar^2}{2}\sum_i (\mathbf{M}_h^{-1})_{ii} k_i^2. \tag{9.7}$$

We can redefine the electron and hole masses by rewriting Eqs. (9.6) and (9.7) as

$$\varepsilon_e(\mathbf{k}) = \varepsilon_c + \frac{\hbar^2}{2}\sum_{i=1}^{3} \frac{1}{m_i^e} k_i^2 \tag{9.8}$$

and

$$\varepsilon_h(\mathbf{k}) = \varepsilon_v - \frac{\hbar^2}{2}\sum_{i=1}^{3} \frac{1}{m_i^h} k_i^2. \tag{9.9}$$

9.3 ELECTRON AND HOLE DENSITIES IN EQUILIBRIUM

To determine the number of carriers in each band in a semiconductor, we will modify the expression between the electron density and the density of states derived in Eq. (3.58), which was obtained for free electrons,

$$n = \int_{-\infty}^{\infty} g(\varepsilon) f(\varepsilon) d\varepsilon. \tag{9.10}$$

Here, $f(\varepsilon)$ is the Fermi distribution function, which for electrons is

$$f_e(\varepsilon) = \frac{1}{e^{(\varepsilon-\mu)/k_B T} + 1}. \tag{9.11}$$

In the case of free electrons, the chemical potential μ at $T = 0$ is equal to the Fermi energy ε_F, which is defined as the energy at the boundary between the filled and the empty states. In the case of semiconductors, the filled and empty states are separated by an energy gap E_g. Thus, we can argue that the chemical potential μ, known as the Fermi level in the case of semiconductors, lies somewhere between the energy gap. Later, we will show that for an intrinsic semiconductor, the Fermi level lies exactly at the middle of the gap at $T = 0$. In addition, we are considering the density of electrons in the conduction band for which Eq. (9.10) is modified as

$$n_c(T) = \int_{\varepsilon_c}^{\infty} g_c(\varepsilon) f_e(\varepsilon) d\varepsilon, \tag{9.12}$$

where $g_c(\varepsilon)$ is the density of states of the electrons in the conduction band. We can write a similar expression for the holes in the valence band except that the distribution function for a hole can be written as

$$f_h(\varepsilon) = 1 - \frac{1}{e^{(\varepsilon-\mu)/k_BT}+1} = \frac{1}{e^{(\mu-\varepsilon)/k_BT}+1}. \tag{9.13}$$

In addition, the density of states for holes lies below the valence band edge. Thus, the density of holes in the valence band can be written as

$$p_v(T) = \int_{-\infty}^{\varepsilon_v} g_v(\varepsilon) f_h(\varepsilon) d\varepsilon, \tag{9.14}$$

where $g_v(\varepsilon)$ is the density of states of the holes in the valence band. For semiconductors, the conduction bands are nearly empty, and the valence bands are nearly full. We assume that the band shapes are nearly parabolic as in the case of free electrons. Therefore, we use the expression for the density of states for a free electron gas derived in Eq. (3.56) and suitably modify it for semiconductors by substituting effective masses m_n^* and m_p^* for the free electron mass m, and the fact that the energy of the electrons is $\varepsilon \geq \varepsilon_c$ and the energy of the holes is $|\varepsilon| \leq \varepsilon_v$ (we note that the energy of the holes is negative),

$$\begin{aligned} g_c(\varepsilon) &= \frac{\sqrt{2m_n^{*3}\varepsilon'}}{\pi^2\hbar^3}\eta_c, \quad && \varepsilon' > \varepsilon_c \\ &= 0, && \varepsilon' \leq \varepsilon_c, \end{aligned} \tag{9.15}$$

where

$$\varepsilon' \equiv \varepsilon - \varepsilon_c, \tag{9.16}$$

and

$$\begin{aligned} g_v(\varepsilon) &= \frac{\sqrt{2m_p^{*3}|\varepsilon''|}}{\pi^2\hbar^3}, \quad && |\varepsilon''| > \varepsilon_v \\ &= 0, && |\varepsilon''| \leq \varepsilon_v, \end{aligned} \tag{9.17}$$

where

$$|\varepsilon''| \equiv |\varepsilon - \varepsilon_v|. \tag{9.18}$$

Here, η_c is the number of symmetrically equivalent minima in the conduction band (six for Si and eight for Ge). m_n^* and m_p^* are the effective mass of electrons and holes that are obtained from the relation

$$m_n^* = (m_1^e m_2^e m_3^e)^{1/2} \tag{9.19}$$

and

$$m_p^{*3/2} = (m_{pl}^*)^{3/2} + (m_{ph}^*)^{3/2}, \tag{9.20}$$

where

$$m_{pl}^{*} = (m_1^{lh} m_2^{lh} m_3^{lh})^{1/2} \tag{9.21}$$

and

$$m_{ph}^{*} = (m_1^{hh} m_2^{hh} m_3^{hh})^{1/2}. \tag{9.22}$$

Here, m_{pl}^{*} and m_{ph}^{*} are the effective masses of the light and heavy holes defined in Eqs. (9.15) and (9.17), respectively. We note that in Eq. (9.17), the energy of the holes is zero at the valence band and negative downwards.

For most semiconductors, the following approximations can be easily made:

$$\varepsilon_c - \mu \gg k_B T \tag{9.23}$$

and

$$\mu - \varepsilon_v \gg k_B T. \tag{9.24}$$

The semiconductors for which the approximations (9.23) and (9.24) are valid are known as nondegenerate semiconductors, whereas those for which these approximations are not valid are known as degenerate semiconductors and one has to use Eqs. (9.11) and (9.13) for $f_e(\varepsilon)$ and $f_h(\varepsilon)$, respectively. For nondegenerate semiconductors, we can rewrite Eqs. (9.11) and (9.13) as

$$f_e(\varepsilon) \approx e^{-(\varepsilon-\mu)/k_B T} \approx e^{[-\varepsilon_c-(\varepsilon'-\mu)]/k_B T} \approx e^{-\varepsilon_c/k_B T} f_e(\varepsilon') \tag{9.25}$$

and

$$f_h(\varepsilon) \approx e^{(\varepsilon-\mu)/k_B T} \approx e^{[\varepsilon_v+(|\varepsilon-\varepsilon_v|-\mu)]/k_B T} \approx e^{\varepsilon_v/k_B T} f_h(|\varepsilon''|). \tag{9.26}$$

The density of carriers (in the conduction and valence bands) is obtained from the relations,

$$n_c(T) = \int_0^{\infty} g_c(\varepsilon') f_e(\varepsilon') d\varepsilon' \tag{9.27}$$

and

$$p_v(T) = \int_0^{\infty} g_v(|\varepsilon''|) f_h(|\varepsilon''|) d|\varepsilon''|. \tag{9.28}$$

From Eqs. (9.15), (9.25), and (9.27), the expression for $n_c(T)$ is obtained as

$$n_c(T) = \eta_c \frac{\sqrt{2m_n^{*3}}}{\pi^2 \hbar^3} e^{(\mu-\varepsilon_c)/k_B T} \int_0^{\infty} \varepsilon'^{1/2} e^{-\varepsilon'/k_B T} d\varepsilon'. \tag{9.29}$$

From Eqs. (9.17), (9.26), and (9.28), the expression for $p_v(T)$ is obtained as

$$p_v(T) = \frac{\sqrt{2m_p^{*3}}}{\pi^2 \hbar^3} e^{(\varepsilon_v-\mu)/k_B T} \int_0^{\infty} |\varepsilon''|^{1/2} e^{-|\varepsilon''|/k_B T} d|\varepsilon''|. \tag{9.30}$$

It can be easily shown that

$$\int_0^\infty \varepsilon^{1/2} e^{-\varepsilon/k_B T} d\varepsilon = \frac{1}{2}(k_B T)^{3/2} \pi^{1/2}. \tag{9.31}$$

From Eqs. (9.29) and (9.31), we obtain

$$n_c(T) = \aleph_c(T) e^{(\mu - \varepsilon_c)/k_B T} \tag{9.32}$$

where

$$\aleph_c(T) = 2\eta_c \left(\frac{m_n^* k_B T}{2\pi\hbar^2} \right)^{3/2}. \tag{9.33}$$

$\aleph_c(T)$ can be expressed numerically as

$$\aleph_c(T) = 2.51\eta_c \left(\frac{m_n^*}{m} \right)^{3/2} \left(\frac{T}{300\ \text{K}} \right)^{3/2} \times 10^{19} \text{cm}^{-3}. \tag{9.34}$$

Similarly, from Eqs. (9.30) and (9.31), we obtain

$$p_v(T) = \wp_v(T)\ e^{(\varepsilon_v - \mu)/k_B T}, \tag{9.35}$$

where

$$\wp_v(T) = 2\left(\frac{m_p^* k_B T}{2\pi\hbar^2} \right)^{3/2}. \tag{9.36}$$

$\wp_v(T)$ can be expressed numerically as

$$\wp_v(T) = 2.51 \left(\frac{m_p^*}{m} \right)^{3/2} \left(\frac{T}{300\ \text{K}} \right)^{3/2} 10^{19} \text{cm}^{-3}. \tag{9.37}$$

From Eqs. (9.32) and (9.35), we obtain

$$n_c(T) p_v(T) = \aleph_c(T) \wp_v(T) e^{-E_g/k_B T}, \tag{9.38}$$

where E_g is the energy gap between the conduction and valence band,

$$E_g = \varepsilon_c - \varepsilon_v. \tag{9.39}$$

Eq. (9.38) is known as the *law of mass action*. It states that at a given temperature, one can obtain the density of one type of carrier if one knows the density of the other type of carrier, the effective masses of both carriers (including that of light and heavy holes), the number of symmetrically equivalent minima in the conduction band, and the energy gap of the semiconductor.

We note that Eqs. (9.32) and (9.35) are valid for both intrinsic (pure) and extrinsic (semiconductors with natural or doped impurities) semiconductors. We will first consider the case of intrinsic semiconductors.

9.4 INTRINSIC SEMICONDUCTORS

In an intrinsic semiconductor, because the number of electrons $n_c(T)$ in the conduction band is equal to the number of holes $p_v(T)$ in the valence band, we can express n_i, the number of carriers in each band from Eq. (9.38), as

$$n_i(T) = \sqrt{n_c(T)p_v(T)} = \sqrt{\aleph_c(T)\wp_v(T)}\, e^{-E_g/2k_BT}. \tag{9.40}$$

From Eqs. (9.34), (9.37), and (9.40), we obtain

$$n_i(T) = 2.51\eta_c^{1/2}\left(\frac{m_n^* m_p^*}{m^2}\right)^{3/4}\left(\frac{T}{300\ \text{K}}\right)^{3/2} e^{-E_g/2k_BT}10^{19}\ \text{cm}^{-1}. \tag{9.41}$$

The chemical potential of an intrinsic semiconductor is obtained from the equality relation

$$n_i(T) = n_c(T) = p_v(T), \tag{9.42}$$

and from Eqs. (9.32) and (9.35),

$$\aleph_c(T)e^{(\mu_i-\varepsilon_c)/k_BT} = \wp_v(T)e^{(\varepsilon_v-\mu_i)/k_BT} \tag{9.43}$$

or

$$\mu = \mu_i = \varepsilon_v + \frac{1}{2}E_g + \frac{1}{2}k_BT\ln\frac{\wp_v(T)}{\aleph_c(T)}. \tag{9.44}$$

From Eqs. (9.33), (9.36), and (9.44), we obtain

$$\mu_i = \varepsilon_v + \frac{1}{2}E_g + \frac{3}{4}k_BT\ln\left(\frac{m_p^*}{m_n^*}\right) - \frac{1}{2}k_BT\ln\eta_c. \tag{9.45}$$

From Eq. (9.45), at $T = 0$, μ_i has a simple form,

$$\mu_i = \varepsilon_v + \frac{1}{2}E_g, \tag{9.46}$$

which is precisely at the center of the energy gap. Even at reasonable temperatures, because $m_p^* \approx m_n^*$ for most semiconductors, μ_i is close to the center of the energy gap. This is shown in Figure 9.3.

From Eq. (9.32) and in analogy with the free electron model, we can write the conductivity σ_i of an intrinsic semiconductor as

$$\sigma_i = \frac{n_i e^2\tau_e}{m_n^*} + \frac{p_i e^2\tau_h}{m_p^*}, \tag{9.47}$$

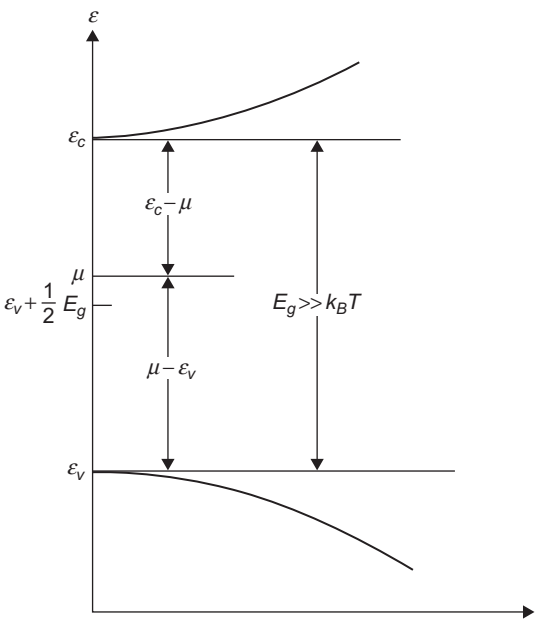

FIGURE 9.3

The chemical potential for an intrinsic semiconductor lies within the energy gap at $T \neq 0$.

where τ_e and τ_h are the relaxation times for electrons and holes. Eq. (9.47) can be rewritten in the alternate and more familiar form

$$\sigma_i = n_i e\mu_e + p_i e\mu_h, \tag{9.48}$$

where μ_e and μ_h are the mobility of the electrons and holes, which is the velocity (always defined as positive) of the carriers in unit electric field.

9.5 EXTRINSIC SEMICONDUCTORS

If there are impurities present in a semiconductor, which contribute a significant number of electrons to the conduction band or holes to the valence band, the semiconductor is known as an extrinsic semiconductor. This can be obtained either by doping (which is the base of modern electronics) or by contamination. In either case,

$$\Delta n(T) = n_c(T) - p_v(T) \neq 0. \tag{9.49}$$

From Eqs. (9.38) and (9.40), we have

$$n_c(T)p_v(T) = n_i(T)^2, \tag{9.50}$$

which can be rewritten in the alternate form (dropping the T in the bracket),

$$(p_v + \Delta n)p_v = n_i^2, \tag{9.51}$$

or

$$p_v^2 + \Delta n p_v - n_i^2 = 0. \tag{9.52}$$

Solving the quadratic equation, we have

$$p_v = -\frac{1}{2}\Delta n + \frac{1}{2}\left[(\Delta n)^2 + 4n_i^2\right]^{\frac{1}{2}}. \tag{9.53}$$

Following a similar procedure, we obtain

$$n_c = \frac{1}{2}\Delta n + \frac{1}{2}\left[(\Delta n)^2 + 4n_i^2\right]^{\frac{1}{2}}. \tag{9.54}$$

We dropped the negative sign before the square root in Eqs. (9.53) and (9.54) because both p_v and n_c are positive. We also obtain from Eqs. (9.32), (9.35), and (9.42),

$$n_c = n_i e^{(\mu-\mu_i)/k_B T} \tag{9.55}$$

and

$$p_v = p_i e^{-(\mu-\mu_i)/k_B T} = n_i e^{-(\mu-\mu_i)/k_B T}. \tag{9.56}$$

From Eqs. (9.49), (9.55), and (9.56), we have

$$n_c - p_v = n_i[e^{(\mu-\mu_i)/k_BT} - e^{-(\mu-\mu_i)/k_BT}] = 2n_i \sinh[(\mu-\mu_i)/k_BT]. \tag{9.57}$$

From Eqs. (9.49) and (9.57), we obtain

$$\frac{\Delta n}{n_i} = 2\sinh[(\mu-\mu_i)/k_BT], \tag{9.58}$$

which can be expressed in the alternate form

$$\mu = \mu_i + k_BT \sinh^{-1}\left[\frac{\Delta n}{2n_i}\right]. \tag{9.59}$$

Because μ_i is at the center of the energy gap, Δn must exceed n_i by many orders of magnitude before the chemical potential μ violates the condition of "nondegeneracy" stated earlier (Eqs. 9.23 and 9.24). The exception is in a region of "extreme extrinsic behavior."

We also note from Eqs. (9.53) and (9.54), if $|\Delta n| \gg n_i$, and if Δn is positive,

$$n_c \approx \Delta n \text{ and } p_v \approx n_c\left(\frac{n_i}{\Delta n}\right)^2, \tag{9.60}$$

in which case, $n_c \gg p_v$ and the semiconductor is called n-type. If Δn is negative,

$$p_v \approx |\Delta n| \text{ and } n_c \approx p_v\left(\frac{n_i}{|\Delta n|}\right)^2, \tag{9.61}$$

in which case, $p_v \gg n_c$ and the semiconductor is called p-type. These types of semiconductors are known as doped semiconductors and are the base on which modern electronics is built.

9.6 DOPED SEMICONDUCTORS

Doped impurities, which contribute additional electrons to the conduction band such that the semiconductor becomes n-type, are known as donors, whereas those that contribute holes to the valence band to make the semiconductor p-type are known as acceptors. The simplest example is that when in a group IV semiconductor such as a crystal of pure Si, an Si atom is replaced with a P atom, and there is an extra electron (because phosphorous has five valence electrons) that does not participate in the covalent bonds of Si. A deliberate substitution of quite a large number of P in Si is called doping, and because the excess electrons that are originally bound to their parent phosphorus atoms eventually end up in the conduction band at room temperature (because, as we will show, this binding energy is small), the semiconductor is called the n-type. A schematic diagram of this type of doping is shown in Figure 9.4.

The problem of the substitutional impurity can be simplified by ignoring the structural difference between silicon and phosphorus ion cores. In addition, as shown in Figure 9.5, the extra electron, which is bound to the parent phosphorus atom, can essentially be considered as a particle of charge $-e$ and mass m^* moving in the presence of an attractive center of charge e in a medium of dielectric constant $\in$. This problem is equivalent to that of the ground state of a hydrogen atom with two modifications: the dielectric constant $\in_0$ of a vacuum (in a hydrogen atom) is replaced by the dielectric constant $\in$ of the semiconductor, and the free electron mass (m_e) is replaced by the effective mass m_e^*.

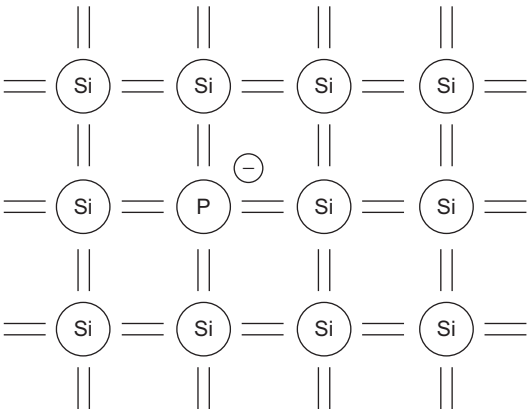

FIGURE 9.4

Phosphorus atom in a pure silicon crystal (donor impurity).

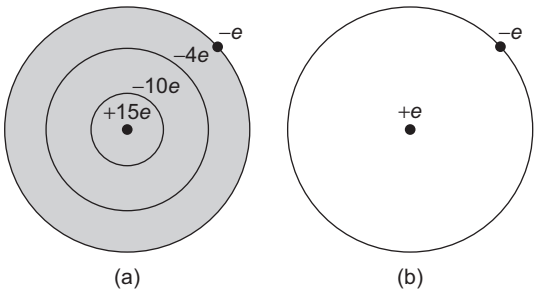

FIGURE 9.5

(a) The electrons in a phosphorus impurity. (b) The 10 inner electrons and the 4 valence electrons, which participate in the covalent bonding, screen the nucleus, which has an effective attractive charge e.

The binding energy of the donor electron is given by

$$\varepsilon = -\frac{m_e^* e^4}{2(4\pi \in \hbar)^2}, \tag{9.62}$$

and the radius of the first Bohr orbit is given by

$$r = \frac{m}{m_e^*} \in a_0, \tag{9.63}$$

where a_0 is the first Bohr radius and m is the free electron mass. Because the dielectric constant $\in$ is large ($\sim$20) and the effective mass m_e^* is small ($\sim$0.1 m), $r \sim 100$ A°. This justifies the use of a semiclassical model, and the binding energy is obtained from the expression

$$\varepsilon \approx \frac{m_e^*}{m} \frac{1}{\in^2} \times 13.6 \text{ eV}. \tag{9.64}$$

Using the same arguments, one can easily show that the binding energy of the donor electron is $\sim -0.01\ 5$ eV. The bound impurity level is formed relative to the energy of the conduction band, and hence, the binding energy, which is much smaller than the energy gap ($(E_g \approx 1.14$ eV for Si), is measured relative to these levels. At room temperature, the donor impurity is ionized, and the electron jumps to the conduction band. When a large number of such extra electrons are introduced in the conduction band by doping Si with P (or other elements from group V), the crystal is known as an n-type semiconductor.

It is easy to make the same argument for acceptor impurities by substituting an Si atom with an element from group III in a silicon crystal. An example of substituting an Si atom with an Al atom in a silicon crystal is shown in Figure 9.6.

As shown in Figure 9.6, there is a deficiency of one electron in the formation of a covalent bond that requires four electrons while aluminum has only three valence electrons. Thus, a hole is created

that is initially bound to the parent aluminum atom. This bound state is known as an acceptor state with a role reversal of a hydrogen-like atom in the sense that there is a net charge of '$-e$' and mass m at the center and hole with charge 'e' and effective mass m_h^* orbiting around it. One can easily show that the radius of the first Bohr orbit is given by

$$r_h = \frac{m}{m_h^*} \in a_0. \tag{9.65}$$

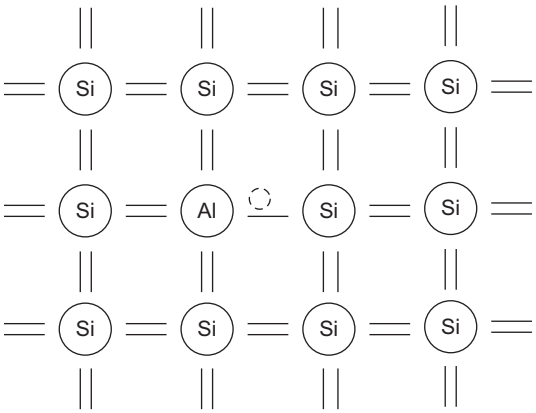

FIGURE 9.6

An example of acceptor impurity: aluminum atom in a silicon crystal.

The binding energy of the ground state is nearly the same for both electrons and holes, i.e., on the order of −0.015 eV. However, the binding energy of the donor levels is measured relative to the conduction band, and the binding energy of the acceptor levels is measured relative to the valence band (the zero of the valence band is at the top of the band, and the energy of the holes is measured positive downwards). Thus, both the donor and the acceptor levels are formed in the energy gap, as shown in Figure 9.7.

However, at room temperature, the thermal energy is sufficient for both the electrons and holes to fall into the conduction and valence bands, respectively.

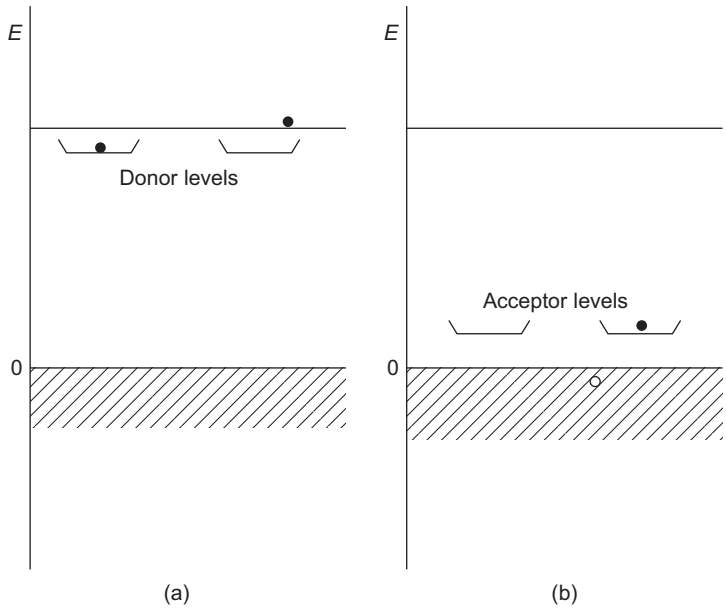

FIGURE 9.7

Donor and acceptor levels for (a) *n*-type and (b) *p*-type semiconductors.

9.7 STATISTICS OF IMPURITY LEVELS IN THERMAL EQUILIBRIUM

9.7.1 Donor Levels

For simplicity, we consider a semiconductor with donor states that have a binding energy ε_d located just below the bottom of the conduction band. Ignoring electron–electron interaction, the three possibilities for the donor level are either the level could be empty, or the donor could trap one electron of either spin (up or down). The donor level cannot bind two electrons of opposite spin at the same time. Using the Fermi statistics (in a grand canonical ensemble), we obtain f_d, the mean number of electrons in the donor level,

$$f_d = \frac{\sum_i n_i e^{-\beta(\varepsilon_i - \mu N_i)}}{\sum_i e^{-\beta(\varepsilon_i - \mu N_i)}}, \tag{9.66}$$

which can be written in the form

$$f_d = \frac{0 + 2e^{-\beta(\varepsilon_d - \mu)}}{1 + 2e^{-\beta(\varepsilon_d - \mu)}}. \tag{9.67}$$

A more appropriate way to write Eq. (9.67) is

$$f_d = \frac{1}{1 + \frac{1}{2}e^{\beta(\varepsilon_d - \mu)}}. \tag{9.68}$$

If the density of donors per unit volume is N_d, we can express n_d, the number density of electrons bound to the donor sites $(n_d = N_d f_d)$, as

$$n_d = \frac{N_d}{1 + \frac{1}{2}e^{\beta(\varepsilon_d - \mu)}}. \tag{9.69}$$

9.7.2 Acceptor Levels

The statistics of the holes can be simplified by considering the holes as the "absence" of electrons. An acceptor level, which is placed at an energy ε_a above the valence band, can be either singly or doubly occupied but cannot be empty. An acceptor impurity is essentially a fixed, negatively charged $(-e)$ attractive center superimposed on an unaltered host atom, which can weakly bind one hole. The binding energy of the hole is $\varepsilon_a - \varepsilon_v$, and a second electron moves into the acceptor level when the hole is "ionized." There is little probability that two holes would be localized in the presence of the acceptor impurity because the Coulomb repulsion between two holes would be very large. This scenario corresponds to no electrons in the acceptor level. In addition, we must account for the fact that the valence maximum is four-fold degenerate (including spin degeneracy). Thus, we obtain an expression for f'_d, the occupation probability of electrons in the acceptor level,

$$f'_d = \frac{4e^{\beta\mu} + 2e^{-\beta(\varepsilon_a - 2\mu)}}{4e^{\beta\mu} + e^{-\beta(\varepsilon_a - 2\mu)}} = \frac{1 + \frac{1}{2}e^{\beta(\mu - \varepsilon_a)}}{1 + \frac{1}{4}e^{\beta(\mu - \varepsilon_a)}}. \tag{9.70}$$

The average number of holes in the acceptor level is the difference between the maximum number of electrons the level can hold (two) and the mean number of electrons in the level, which can be rewritten in the alternate form (for the mean number of holes)

$$f_a = 2 - f_d' = 2 - \frac{1 + \frac{1}{2}e^{\beta(\mu-\varepsilon_a)}}{1 + \frac{1}{4}e^{\beta(\mu-\varepsilon_a)}} = \frac{1}{1 + \frac{1}{4}e^{\beta(\mu-\varepsilon_a)}}. \tag{9.71}$$

If the semiconductor is doped with N_a acceptor impurities per unit volume, $p_a (p_a = N_a f_a)$, the number of holes in the acceptor levels is

$$p_a = \frac{N_a}{1 + \frac{1}{4}e^{\beta(\mu-\varepsilon_a)}}. \tag{9.72}$$

9.7.3 Doped Semiconductors

We assume that a semiconductor is doped with N_d donor impurities and N_a acceptor impurities (per unit volume) and assume that $N_d \geq N_a$. Thus, N_a of the N_d electrons, which are supplied by the donor atoms, will drop from the donor levels into the acceptor levels. The eventual scenario is that in the ground state ($T = 0$), both the valence band and the acceptor levels are filled. In addition, $N_d - N_a$ of the donor levels are filled, but the conduction bands are empty. However, at finite temperature, the number of empty (electron) levels is $p_a + p_v$ in the valence band and the acceptor levels. So, we can write

$$N_d - N_a = n_c + n_d - p_v - p_a, \tag{9.73}$$

where n_c and n_d are the number of electrons in the conduction band and donor levels. To simplify the formulation, we assume (known as the conditions of nondegeneracy) that

$$\varepsilon_d - \mu \gg k_B T \tag{9.74}$$

and

$$\mu - \varepsilon_a \gg k_B T. \tag{9.75}$$

From Eqs. (9.69), (9.70), (9.74), and (9.75), we conclude that the impurities are essentially ionized and hence $n_d \ll N_d$ and $p_a \ll N_a$. Therefore, Eq. (9.74) can be approximated as

$$N_d - N_a \approx n_c - p_v \approx \Delta n. \tag{9.76}$$

From Eqs. (9.53), (9.54), and (9.76), we obtain

$$n_c = \frac{1}{2}[(N_d - N_a)] + \frac{1}{2}[(N_d - N_a)^2 + 4n_i^2]^{\frac{1}{2}} \tag{9.77}$$

and

$$p_v = \frac{1}{2}[(N_a - N_d)] + \frac{1}{2}[(N_d - N_a)^2 + 4n_i^2]^{\frac{1}{2}}. \tag{9.78}$$

In addition, Eq. (9.59) can be rewritten in the alternate form

$$\mu = \mu_i + k_B T \sinh^{-1}(|N_d - N_a|/2n_i). \tag{9.79}$$

Thus, $|N_d - N_a|$ must exceed n_i by many orders of magnitude before the conditions of nondegeneracy outlined in Eqs. (9.74) and (9.75) are violated. From Eqs. (9.69) and (9.72), we obtain $n_d \approx N_d$ and $p_a \approx N_a$, thereby ensuring that most of the impurities are fully ionized. From Eq. (9.77), we obtain in the extrinsic regime ($n_i \ll |N_d - N_a|$), when $N_d \gg N_a$,

$$n_c \approx N_d - N_a \tag{9.80}$$

and

$$p_v \approx \frac{n_i^2}{N_d - N_a}. \tag{9.81}$$

Eqs. (9.80) and (9.81) state that the number of donors is essentially equal to the number of mobile electrons while the number of holes in the valence band is very small. In the other extrinsic regime, when $N_a \gg N_d$, we obtain from Eq. (9.78),

$$p_v \approx N_a - N_d \tag{9.82}$$

and

$$n_c \approx \frac{n_i^2}{N_a - N_d}. \tag{9.83}$$

Eqs. (9.82) and (9.83) state that the number of acceptors is essentially equal to the number of mobile holes in the valence band while the number of electrons in the conduction band is very small.

9.8 DILUTED MAGNETIC SEMICONDUCTORS

9.8.1 Introduction

The diluted magnetic semiconductors (DMSs), which are ternary or quaternary alloys, in which a part of the nonmagnetic cations of the host material has been substituted by magnetic ions, have attracted considerable attention in recent years. In theory, any semiconductor with a fraction of its constituent ions replaced by ions bearing a net magnetic moment is considered as a DMS. However, in practice, the majority of DMS involve Mn^{2+} ions embedded in various $A^{II}B^{VI}$ or $A^{IV}B^{VI}$ hosts because Mn^{2+} can be incorporated in the host without affecting the crystallographic quality of the resulting material. In addition, Mn^{2+} possesses a relatively large magnetic moment characteristic of a half-filled d-shell ($S = 5/2$). Further, because Mn^{2+} is electrically neutral in $A^{II}B^{VI}$ or $A^{IV}B^{VI}$ hosts, it does not have accepting or donating centers. The Mn containing IV–VI DMSs can be divided into two groups, according to their carrier concentrations. The magnetic behavior of the first group (charge–carrier concentration, or p-type, range $10^{17}-10^{19}\text{cm}^{-3}$) can be ascribed to antiferromagnetic interactions of the superexchange type between the Mn ions. This group has a spin-glass phase at low temperatures. The magnetic behavior of the second group (charge-carrier concentration, or p, of 10^{21}cm^{-3}) has a ferromagnetic ordering,

induced by RKKY interactions (an indirect exchange mechanism in which the interaction between the magnetic ions is mediated by the itinerant charge carriers, or p) at low temperatures.

The magnetic properties of $Sn_{1-x}Mn_xTe$ and $Pb_{0.28-x}Sn_{0.72}Mn_xTe$ (which can be considered as partly like semimetals and partly like semiconductors) are very diverse. The ferromagnetic, spin-glass (SG) and reentrant-spin-glass phases have been observed, but the transition to a paramagnetic phase has not been observed at $T > 1.5$ K. The occurrence of these magnetic phases depends not only on the Mn concentration but also on the concentration of free carriers. The significance of carrier-mediated magnetism in a DMS is mainly due to the search for materials suitable for information processing and storage (in the light of developments in the rapidly emerging area of spintronics, which will be discussed in Chapter 11).

Some experimental results of the three-dimensional (T, x, p) magnetic phase diagram for $Sn_{1-x}Mn_xTe$ are shown in Figure 9.8.

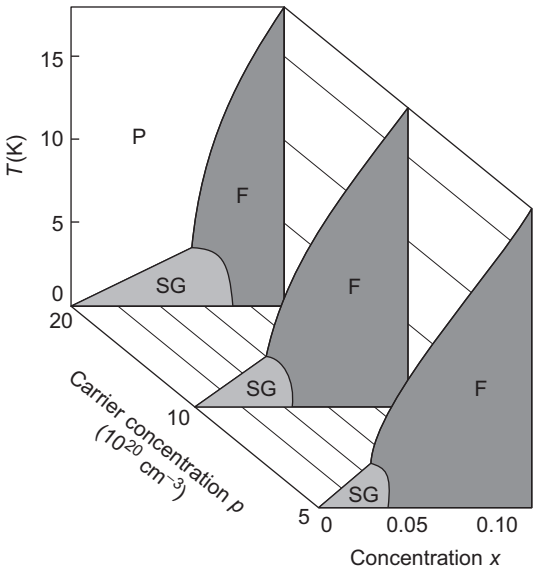

FIGURE 9.8

(T, x, p) phase diagram for $Sn_{1-x}Mn_xTe$.
F = ferromagnetic phase; P = paramagnetic phase; SG = spin-glass phase.

Reproduced from Vennix et al.,[18] with the permission of the American Physical Society.

In subsequent experiments, the magnetic phase of the samples included magnetization, AC susceptibility, specific heat, and neutron diffraction. In Figure 9.9, the magnetic phase is displayed as a function of both the Mn concentration and the carrier concentration. The carrier concentration (the theoretical calculation of which is described later) has a significant effect on the magnetic phase of the material. At a carrier concentration of $p_c = 3 \times 10^{20}\,\text{cm}^{-3}$ ($T > 1.5$ K), there is an abrupt change from the paramagnetic to ferromagnetic phase. At high carrier concentrations $(p \gg p_c)$, there is a gradual transition to an intermediate reentrant-spin-glass phase and eventually to the spin-glass state. The location of these transitions is shifted to higher carrier concentrations if the Mn concentration is increased.

9.8.2 Magnetization in Zero External Magnetic Field in a DMS

Another interesting property of some DMSs is that magnetization in a zero external magnetic field can be induced by optically excited carriers in $Hg_{1-x}Mn_xTe$ and $Cd_{1-x}Mn_xTe$. The observed magnetization is due to the orientation of the Mn ions caused by the spin dynamics of the magnetic response on a picosecond time scale and is the result of spin-polarized electrons. This can be calculated by the spin-EPR shift, of which the theory is briefly described.

9.8.3 Electron Paramagnetic Resonance Shift

The electron paramagnetic resonance (EPR) shift is a measure of the internal field created at the magnetic ion site in magnetic materials or materials with magnetic impurities by the partial

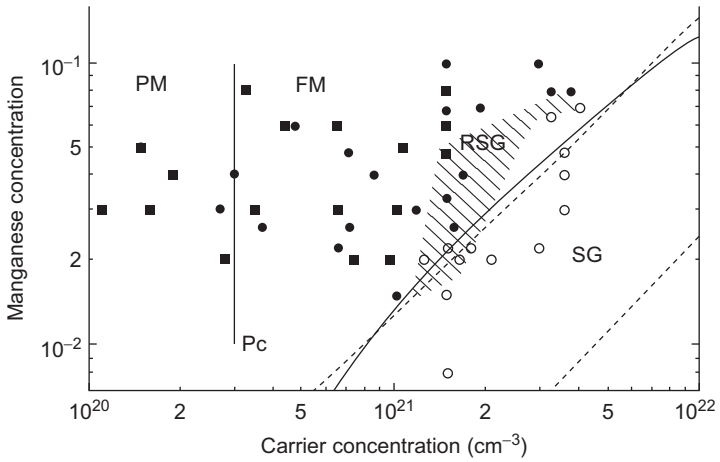

FIGURE 9.9

Magnetic-phase diagram of $Pb_{0.28-x}Sn_{0.72}Mn_xTe$ (squares) and $Sn_{1-x}Mn_xTe$ (circles). PM = paramagnetic, FM = ferromagnetic, RSG = reentrant spin glass, SG = spin glass.

Reproduced from Eggenkamp et al.,[5] with the permission of the American Physical Society.

polarization of electrons and/or carriers in an applied magnetic field. It can be shown that the contribution to the spin-EPR shift at the Mn^{2+} ion on the *j*th site of a DMS ($P_j^{\mu\nu}$) is given by the expression

$$P_j^{\mu\nu} = -\frac{\partial^2 \Omega}{\partial B^\mu \partial M_j^\nu}\Big|_{\vec{B}\to 0, \vec{M}_j \to 0}, \tag{9.84}$$

where Ω is the thermodynamic potential and is given by

$$\Omega = \frac{1}{\beta} Tr \ln(-\widetilde{G}_{\xi_l}). \tag{9.85}$$

Here, $\vec{M}_j$ is the local moment at the *j*th site, and $\widetilde{G}$ is related to the one-particle Green's function (Eq. 7.219) in the presence of a periodic potential $V(\vec{r})$, spin-orbit interaction, applied magnetic field $\vec{B}$, and local magnetic moment. *Tr* involves summation of over both imaginary frequencies and one-particle states, forming a complete orthonormal set. The one-particle Green's function $G(\vec{r}, \vec{r'}, \vec{B}, \vec{M}_j, \xi_l)$ satisfies the equation

$$(\xi_l - H)G(\vec{r}, \vec{r'}, \vec{B}, \vec{M}_j, \xi_l) = \delta(\vec{r} - \vec{r'}), \tag{9.86}$$

where the complex energy

$$\xi_l = \frac{(2l+1)i\pi}{\beta} + \mu, \quad l = 0, \pm 1, \pm 2, \ldots, \tag{9.87}$$

and in a symmetric gauge,

$$G(\vec{r}, \vec{r}, \vec{B}, \vec{M}_j, \xi_l) = e^{i\vec{h}\cdot\vec{r}\times\vec{r'}} \widetilde{G}(\vec{r}, \vec{r'}, \vec{B}, \vec{M}_j, \xi_l), \tag{9.88}$$

where

$$\overrightarrow{h} = \frac{e\overrightarrow{B}}{2\hbar c}. \tag{9.89}$$

Here, $\widetilde{G}$ is the Green's function that satisfies the lattice translational symmetry, and $e^{i\overrightarrow{h}\cdot\overrightarrow{r}\times\overrightarrow{r'}}$ is the Peierls phase factor. The phase factor has the effect of translating the origin of the vector potential.

Recently, Trellakis[16] used a singular gauge transformation based on a lattice of magnetic flux lines, an equivalent quantum system with a periodic vector potential. However, his theory is beyond the scope of this book. The one-particle Hamiltonian is

$$\hat{H} = \frac{1}{2m}(\overrightarrow{p} + \frac{e}{c}\overrightarrow{A})^2 + V(\overrightarrow{r}) + \frac{\hbar}{4m^2c^2}\overrightarrow{\sigma}\cdot\overrightarrow{\nabla}V\times(\overrightarrow{p} + \frac{e}{c}\overrightarrow{A}) + \frac{1}{2}g_0\mu_0\overrightarrow{B}\cdot\overrightarrow{\sigma} + \hat{H}_I, \tag{9.90}$$

where

$$\hat{H}_I = \frac{1}{2g_J\mu_0}\sum_{\overrightarrow{j}}\overrightarrow{M}_j\cdot\overrightarrow{\sigma}\mathfrak{I}(\overrightarrow{r} - \overrightarrow{R}_j). \tag{9.91}$$

Here, $\overrightarrow{A}$ is the magnetic vector potential, $\mathfrak{I}(\overrightarrow{r} - \overrightarrow{R}_j)$ is the strength of the exchange interaction between the conduction electrons and/or the carriers and the local moment at the jth site, and the other symbols have their usual meaning. One can write the equation of motion in a representation defined by the periodic part $u_{\overrightarrow{k}\rho}(\overrightarrow{r})$ of the Bloch function $\psi_{\overrightarrow{k}\rho}(\overrightarrow{r})$, where $\overrightarrow{k}$ is the reduced wave vector and ρ is the spin index.

It has been shown (Misra et al.,[11] p. 1903) that in this representation, Eqs. (9.86), (9.88), (9.90), and (9.91) can be rewritten as

$$[\xi_l - H(\overrightarrow{\kappa})]\widetilde{G}(\overrightarrow{k}, \xi_l) = I, \tag{9.92}$$

where

$$H(\overrightarrow{\kappa}) = H_0(\overrightarrow{k}) + H'(\overrightarrow{\kappa}), \tag{9.93}$$

$$H_0(\overrightarrow{k}) = \frac{1}{2m}(\overrightarrow{p} + \hbar\overrightarrow{k})^2 + V + \frac{\hbar^2}{4m^2c^2}\overrightarrow{\sigma}.\overrightarrow{\nabla}V\times(\overrightarrow{p} + \hbar\overrightarrow{k}), \tag{9.94}$$

$$H'(\overrightarrow{\kappa}) = -i\frac{\hbar}{m}h_{\alpha\beta}\pi^\alpha\nabla_k^\beta + \frac{1}{2}g_0\mu_0\sigma^\mu H^\mu + \frac{1}{2\mu_0}\sum_j\frac{1}{g_j}M_j^\nu\sigma^\nu\mathfrak{I}, \tag{9.95}$$

$$\overrightarrow{\kappa} = \overrightarrow{k} + i\overrightarrow{h}\times\overrightarrow{\nabla}_k, \tag{9.96}$$

$$\overrightarrow{\pi} = \overrightarrow{p} + \frac{\hbar}{4mc^2}\overrightarrow{\sigma}\times\overrightarrow{\nabla}V, \tag{9.97}$$

$h_{\alpha\beta} = \in_{\alpha\beta\mu}h^\mu$, where $\in_{\alpha\beta\mu}$ is the antisymmetric tensor of the third rank, and we follow Einstein summation convention. It may be noted that $\overrightarrow{\kappa}$ (Eq. 9.96) is the Misra–Roth operator. Eq. (9.85) can be further simplified by writing the frequency summation as

$$\Omega = -\frac{1}{2\pi i}tr\oint_c\phi(\xi)\widetilde{G}(\xi)d\xi, \tag{9.98}$$

where

$$\phi(\xi) = -\frac{1}{\beta}\ln[1+e^{-\beta(\mu-\xi)}] \tag{9.99}$$

and the contour c encircles the imaginary axis in a counterclockwise direction. Eq. (9.92) can be solved by using a perturbation expansion of $\widetilde{G}(\overrightarrow{k},\xi)$,

$$\widetilde{G}(\overrightarrow{k},\xi) = \widetilde{G}_0(\overrightarrow{k},\xi) + \widetilde{G}_0(\overrightarrow{k},\xi)H'\widetilde{G}_0(\overrightarrow{k},\xi) + \widetilde{G}_0(\overrightarrow{k},\xi)H'\widetilde{G}_0(\overrightarrow{k},\xi)H'\widetilde{G}_0(\overrightarrow{k},\xi). \tag{9.100}$$

Here, the terms only up to second order are retained because the EPR shift independent of the applied field and the local moment is calculated. In Eq. (9.100), $\widetilde{G}_0(\overrightarrow{k},\xi)$ satisfies the equation

$$[\xi - H_0(\overrightarrow{k})]\widetilde{G}_0(\overrightarrow{k},\xi) = I \tag{9.101}$$

and is diagonal in the basis $u_{\overrightarrow{k}\rho}(\overrightarrow{r})$. Using the identity in Eq. (9.100),

$$\nabla_k^\alpha \widetilde{G}_0(\overrightarrow{k},\xi) = \frac{\hbar}{m}\widetilde{G}_0(\overrightarrow{k},\xi)\pi^\alpha\widetilde{G}_0(\overrightarrow{k},\xi), \tag{9.102}$$

we obtain

$$\widetilde{G}(\overrightarrow{k},\xi) = \sum_j M_j^\nu B^\mu \frac{1}{2g_j}\left[\begin{array}{l}(\widetilde{G}_0\sigma^\mu\widetilde{G}_0\sigma^\nu\mathfrak{I}\widetilde{G}_0 + \widetilde{G}_0\sigma^\nu\mathfrak{I}\widetilde{G}_0\sigma^\mu\widetilde{G}_0) \\ -\frac{i}{m}\varepsilon_{\alpha\beta\mu}(\widetilde{G}_0\pi^\alpha\widetilde{G}_0\pi^\beta\widetilde{G}_0\sigma^\nu\mathfrak{I}\widetilde{G}_0 + \widetilde{G}_0\sigma^\nu\mathfrak{I}\widetilde{G}_0\pi^\alpha\widetilde{G}_0\pi^\beta\widetilde{G}_0)\end{array}\right]. \tag{9.103}$$

Here, $\widetilde{G}_0$ is the compact form of $\widetilde{G}_0(\overrightarrow{k},\xi)$. Eq. (9.98) is evaluated by using Eqs. (9.99) and (9.103). Expressing the contributions of the two terms in Eq. (9.103) to Ω as

$$\Omega = \Omega_1 + \Omega_2, \tag{9.104}$$

we obtain

$$\Omega_1 = \sum_j H^\mu M_j^\nu \sum_{n,\overrightarrow{k},\rho,\rho'}\left[\frac{1}{2g_j}\sigma^\nu\mathfrak{I}\right]_{n\rho,n\rho'}\sigma^\mu_{n\rho',n\rho}f'\left(E_{n\overrightarrow{k}\rho}\right) \tag{9.105}$$

and

$$\Omega_2 = \sum_j H^\mu M_j^\nu \sum_{n,m,\overrightarrow{k},\rho,\rho',\rho''m\neq n}\frac{i}{m}\varepsilon_{\alpha\beta\mu}\frac{\left[\frac{1}{2g_j}\sigma^\nu\mathfrak{I}\right]_{n\rho,n\rho'}\pi^\alpha_{n\rho',m\rho''}\pi^\beta_{m\rho'',n\rho}}{E_{mn}}f'\left(E_{n\overrightarrow{k}\rho}\right), \tag{9.106}$$

where

$$E_{mn} \equiv E_{m\overrightarrow{k}} - E_{n\overrightarrow{k}} \tag{9.107}$$

and

$$H_0 u_{n\overrightarrow{k}\rho}(\overrightarrow{r}) = E_{n\overrightarrow{k}}u_{n\overrightarrow{k}\rho}(\overrightarrow{r}). \tag{9.108}$$

The matrix elements are of the type

$$A_{n\rho,n\rho'} \equiv \int u^*_{n\vec{k}\rho}(\vec{r}) A u_{n\vec{k}\rho}(\vec{r}) d\vec{r}, \tag{9.109}$$

and $f'(E_{n\vec{k}})$ is the first derivative of the Fermi function. The expressions for Ω_1 and Ω_2 derived in Eqs. (9.105) and (9.106) are substituted in Eq. (9.84), and the complex spin-orbit terms are neglected. After considerable algebra, we obtain the expression for the spin contribution to the EPR shift at the jth site,

$$P^{\nu\mu}_{js} = -\frac{1}{2} \sum_{n\vec{k}\rho\rho'} \left(\frac{1}{2g_j} \sigma^\nu \mathfrak{F} \right)_{n\rho,n\rho'} g^\mu_{nn}(\vec{k}) \sigma^\mu_{n\rho',n\rho} f'\left(E_{n\vec{k}} \right), \tag{9.110}$$

where the effective g factor $g^\mu_{nn}(\vec{k})$ is defined as

$$g^\mu_{nn}(\vec{k}) \sigma^\mu_{n\rho',n\rho} = g_0 \sigma^\mu_{n\rho',n\rho} + \frac{2i}{m} \in_{\alpha\beta\mu} \sum_{m\neq n,\rho''} \frac{\pi^\alpha_{n\rho',m\rho''} \pi^\beta_{m\rho'',n\rho}}{E_{mn}}. \tag{9.111}$$

Eq. (9.110) can be used to calculate the EPR shift of any diluted magnetic semiconductor of which the band structure is known.

A brief discussion of the calculation of the EPR shift from Eq. (9.110) by using the $\vec{k} \cdot \vec{\pi}$ model is explained in the next section.

9.8.4 $\vec{k} \cdot \vec{\pi}$ Model

The $\vec{k} \cdot \vec{p}$ model of Luttinger and Kohn[9] (p. 869) was modified by Tripathi et al.[17] (p. 3091) to include the effect of magnetic fields. Their method of calculation is known as the $\vec{k} \cdot \vec{\pi}$ model.

In the Luttinger–Kohn ($\vec{k} \cdot \vec{p}$) model, a complete orthonormal set of functions,

$$\chi_j(\vec{k}, \vec{r}) = e^{i(\vec{k}-\vec{k}_0)\cdot\vec{r}} \psi_j(\vec{k}_0, \vec{r}), \tag{9.112}$$

is defined, where $\vec{k}_0$ is a reference point in the Brillouin zone at which the energy bands and wave functions $\psi_j(\vec{k}_0, \vec{r})$ have been determined. The unknown wave function is expanded as

$$\psi_n(\vec{k}, \vec{r}) = \sum_j A_{nj}(\vec{k}) \chi_j(\vec{k}, \vec{r}). \tag{9.113}$$

In the $\vec{k} \cdot \vec{\pi}$ model, the effective equation of motion is

$$\sum_j \left[\left(E_j(\vec{k}_0) - E_n(\vec{k}) + \frac{\hbar^2(k^2 - k_0^2)}{2m} \right) \delta_{jl} + \frac{\hbar}{m} (\vec{k} - \vec{k}_0) \cdot \vec{\pi}_{lj} \right] A_{nj}(\vec{k}) = 0, \tag{9.114}$$

where

$$\vec{\pi}_{lj} = \frac{(2\pi)^3}{\Omega_c} \int_{cell} d^3r \, u^*_l(\vec{k}_0, \vec{r}) \vec{\pi} \, u_j(\vec{k}_0, \vec{r}). \tag{9.115}$$

There is one equation for each value of the band index l, and the condition for this infinite set of simultaneous, linear, and homogeneous equations to have a nontrivial solution is that the determinant of the coefficients should vanish. A general element of the determinant has the form $H_{jl} - E(\vec{k})\delta_{jl}$, with

$$H_{jl} = \left(E_j(\vec{k}_0) + \frac{\hbar^2}{2m}(k^2 - k_0^2)\right)\delta_{jl} + \frac{\hbar}{m}(\vec{k} - \vec{k}_0)\cdot\vec{\pi}_{lj}. \tag{9.116}$$

One can use Eq. (9.116) to determine the spin contribution to the EPR shift (P_s) of any diluted magnetic semiconductor. An example of using this method to determine the EPR shift of $Pb_{1-x}Mn_xTe$ as a function of carrier concentration can be found in Das et al.[4]

9.9 ZINC OXIDE

The semiconductor ZnO has attracted widespread attention in recent years for its optoelectronic properties and, more recently, for the possibility of finding room-temperature ferromagnetism when doped with magnetic and nonmagnetic impurities. The electronic structure of ZnO has been studied for the past 50 years. However, in spite of extensive energy band calculations, there still exists a controversy with regard to the valence band ordering in ZnO. The wurtzite ZnO conduction band is mainly constructed from the *s*-like state having Γ_7 symmetry, whereas the valence band is *p*-like, which is split into three bands due to the crystal field and spin-orbit interactions. A schematic picture of the band diagram is given in Figure 9.10. By treating the wurtzite energy levels as a perturbation over those of the zincblende, a formula has been derived for the valence band mixing, the extent of which is controlled by the relative magnitudes of the spin-orbit and crystal field splittings.

No satisfactory theory has yet been proposed for the possibility of finding room-temperature ferromagnetism in ZnO, when doped with magnetic and nonmagnetic impurities. Some of the fascinating theoretical models include the $\mathbf{k}\cdot\mathbf{p} + \mathrm{U}$ formalism, where U is the many-body Hubbard term.

9.10 AMORPHOUS SEMICONDUCTORS

9.10.1 Introduction

In recent years, amorphous semiconductors have attracted considerable attention. The amorphous structures can be obtained by rapid cooling from the melt or by evaporation onto a cooled substrate. They can also be obtained by sputtering the components on to a cooled substrate. The evaporation or sputtering of Si or Ge onto substrates held below 300°C produces amorphous films, which are stable up to 425°C. In the amorphous (a) state, the sp^3 covalent bonds are strong in Si and Ge. However, although these bonds exist between nearest neighbors, the

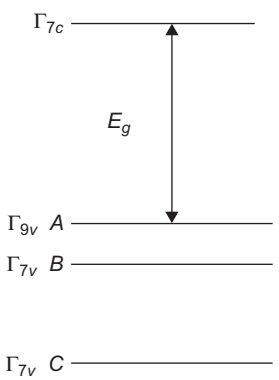

FIGURE 9.10

Schematic picture of valence band ordering for the wurtzite ZnO.

bonding is not perfect. There is four-fold coordination over small regions of the solid, but the tetrahedral symmetry is lost over extended regions. The bond angles are distorted from the ideal value, and many atoms can have only three neighbors. One can consider the system as a random network of imperfectly bonded atoms in which even small voids can exist.

Recent experiments of amorphous semiconductors exhibit many interesting properties. Tetrahedral and quasitetrahedral materials exhibit an unusual enhancement of diamagnetic susceptibility, χ (450% for Si, 270% for Ge, and 150% for $CdGeAs_2$) in the amorphous (a) phase relative to the crystalline (c) phase but no change in dielectric susceptibility (χ_e). In contrast, in chalcogenides, there is very little change in χ in either phase but appreciable reduction of χ_e in the (a) phase. These unusual properties are related to the nature of the chemical bonding and the presence or absence of long-range order. The chemical bond approach to the study of electronic properties of solids is much simpler than the band theory; emphasizes the bond aspect of the crystal structure; and is valuable in studying chemical trends such as covalency, polarity, and metallicity. This approach has a certain degree of flexibility and is well suited to the study of amorphous as well as periodic ones. In the chemical bond approach, each atom in the amorphous system has four nearest neighbors, but the bonds are distorted in bond lengths and directions. Thus, one starts with a crystalline phase and considers the covalent bonds that give rise to bonding and antibonding orbitals, leading to valence and conduction bands. Then distortion in both bond lengths and angles is introduced, and the random network model of Polk[13] (p. 365) is used to derive appropriate expressions for physical properties of amorphous structures.

The electron energy levels of amorphous systems can be derived from a modified bond orbital (LCH) theory typical of the crystalline phase. Even if they are randomly arranged, the covalent bonds give rise to some system of bonding and antibonding levels, which leads to valence and conduction bands. However, due to distortion of the bonds, the bands become broader. We first consider a linear combination of hybrids (LCH) model for tetrahedral semiconductors.

9.10.2 Linear Combination of Hybrids Model for Tetrahedral Semiconductors

We describe a linear combination of hybrids (LCH) model for a chemical bond approach to tetrahedral semiconductors (Sahu and Misra,[14] p. 6795). In this model, the basis set for the valence bands is a linear combination of sp^3 hybrids forming a bond, in which their relative phase factors, which have been neglected in the usual chemical bond models, adapted from the bond orbital models for molecules (Sukhatme and Wolff,[15] p. 1369; Chadi et al.,[2] p. 1372), have been included properly. A basis set for the conduction bands, which are orthogonal to the valence band functions, has also been constructed. It can be shown that the basic assumption of the earlier chemical bond models—i.e., that the localized functions have the character of chemical bonds—is equivalent to ignoring the relative Bloch phase factor $e^{i\mathbf{k}\cdot\mathbf{d}_j}$ (where $\mathbf{d}_j$ is a bond length) between the hybrids forming a bond. However, because $\mathbf{d}_j - \mathbf{d}_{j'} (j \neq j')$ is a lattice vector, these relative phase factors play an important role in solids, unlike the case of molecules where it can be neglected.

We will now discuss the LCH model in detail. In the zincblende structure, each atom is surrounded tetrahedrally by four identical atoms, which may be of the second type. The primitive cell contains two basic atoms at site i, with four sp^3 hybrids $h_j^1(\mathbf{r} - \mathbf{R}_i)$ pointing from atom I to the nearest neighbors (atom II) along the directions $j (j = 1, \ldots, 4)$ and four other sp^3 hybrids $h_j^2(\mathbf{r} - \mathbf{R}_i - \mathbf{d}_j)$ pointing from these nearest neighbors to atom I. Here, $\mathbf{R}_i$ is a lattice vector for site i and locates

atoms of type I (one of the atomic sites I is chosen as the origin) and $\mathbf{d}_j$ is a nearest-neighbor vector joining atom I with atom II. The hybrids can be expressed as

$$h_j^1(\mathbf{r}-\mathbf{R}_i) = \frac{1}{2}[s_1 + \sqrt{3}(\xi_j^x p_{x1} + \xi_j^y p_{y1} + \xi_j^z p_{z1})] \tag{9.117}$$

and

$$h_j^2(\mathbf{r}-\mathbf{R}_i-\mathbf{d}_j) = \frac{1}{2}[s_2 - \sqrt{3}(\xi_j^x p_{x2} + \xi_j^y p_{y2} + \xi_j^z p_{z2})], \tag{9.118}$$

where $\overrightarrow{\xi}_1 = \frac{1}{\sqrt{3}}(1,1,1)$; $\overrightarrow{\xi}_2 = \frac{1}{\sqrt{3}}(1,\overline{1},\overline{1})$; $\overrightarrow{\xi}_3 = \frac{1}{\sqrt{3}}(\overline{1},1,\overline{1})$; and $\overrightarrow{\xi}_4 = \frac{1}{\sqrt{3}}(\overline{1},\overline{1},1)$ are the atomic orbitals at sites I and II, respectively. The Bloch-type tight-binding sums for valence-band basis functions are constructed by taking a linear combination of the hybrids forming a bond

$$\chi_j^v(\mathbf{r},\mathbf{k}) = \sum_i f_j^v(\mathbf{k}) e^{i\mathbf{k}\cdot\mathbf{R}_i}[h_j^1(\mathbf{r}-\mathbf{R}_i) + \lambda h_j^2(\mathbf{r}-\mathbf{R}_i-\mathbf{d}_j)e^{i\mathbf{k}\cdot\mathbf{d}_j}], \tag{9.119}$$

where

$$f_j^v(\mathbf{k}) = [N(1+\lambda^2+2\lambda S\cos\mathbf{k}\cdot\mathbf{d}_j)]^{-1/2}. \tag{9.120}$$

Here, S is the overlap integral, and $\lambda^2/(1+\lambda^2)$ is the probability of the electron being around atom II for III–V semiconductors and is related to Coulson's ionicity (Coulson et al.,[3] p. 357; Nucho et al.,[12] p. 1843) by the expression

$$f_c = \frac{(1-S)^{1/2}(1-\lambda^2)}{(1+\lambda^2+2\lambda S)}. \tag{9.121}$$

We note that the LCH model discussed here is different from the usual bond-orbital model[12] in the sense that a relative phase factor $e^{i\mathbf{k}\cdot\mathbf{d}_j}$ between the two hybrids forming a bond has been included to properly account for the origin.

The basis functions for the conduction band $\chi_j^c(\mathbf{r},\mathbf{k})$ are obtained by constructing functions orthogonal to $\chi_j^v(\mathbf{r},\mathbf{k})$:

$$\chi_j^c(\mathbf{r},\mathbf{k}) = \sum_i f_j^c(\mathbf{k}) e^{i\mathbf{k}\cdot\mathbf{R}_i}[(\lambda + Se^{i\mathbf{k}\cdot\mathbf{d}_j})h_j^1(\mathbf{r}-\mathbf{R}_i) - (\lambda S + e^{i\mathbf{k}\cdot\mathbf{d}_j})h_j^2(\mathbf{r}-\mathbf{R}_i-\mathbf{d}_j)], \tag{9.122}$$

where

$$f_j^c(\mathbf{k}) = \left[\frac{\lambda + Se^{-i\mathbf{k}\cdot\mathbf{d}_j}}{N(1-S^2)(1+\lambda^2+2\lambda S\cos\ \mathbf{k}\cdot\mathbf{d}_j)(\lambda + Se^{i\mathbf{k}\cdot\mathbf{d}_j})}\right]^{1/2}. \tag{9.123}$$

The Bloch eigenfunctions for the valence and conduction bands are

$$\psi_n(\mathbf{r},\mathbf{k}) = \sum_j \alpha_{jn}^v(\mathbf{k})\chi_j^v(\mathbf{r},\mathbf{k}) \tag{9.124}$$

and

$$\psi_m(\mathbf{r},\mathbf{k}) = \sum_j \alpha_{jm}^c(\mathbf{k})\chi_j^c(\mathbf{r},\mathbf{k}), \tag{9.125}$$

where

$$\sum_n \alpha_{jn}^{v}(\mathbf{k})\alpha_{nj'}^{v\dagger}(\mathbf{k}) = \delta_{jj'} \tag{9.126}$$

and

$$\sum_m \alpha_{jm}^{c}(\mathbf{k})\alpha_{mj'}^{c\dagger}(\mathbf{k}) = \delta_{jj'}. \tag{9.127}$$

The conduction and valence bands for the tetrahedral semiconductors as well as the expression for the energy gap can be obtained by using these Bloch functions in the same way they were derived earlier in Chapter 4.

The physical properties of model amorphous semiconductors (a-phase), such as magnetic susceptibility and dielectric constant, are obtained by introducing disorder in the bond angles and the bond lengths. The nearest-neighbor coordinations of the a-phase are not supposed to change appreciably from the c-phase. However, the bands become broader due to distortion of the bonds. In addition, the disorder causes a spread of the energy levels into the energy gap region. These are known as tail states, which arise due to the distorted bonds. These tail states are nonconducting and localized. A schematic picture of these tail states is shown in Figure 9.11.

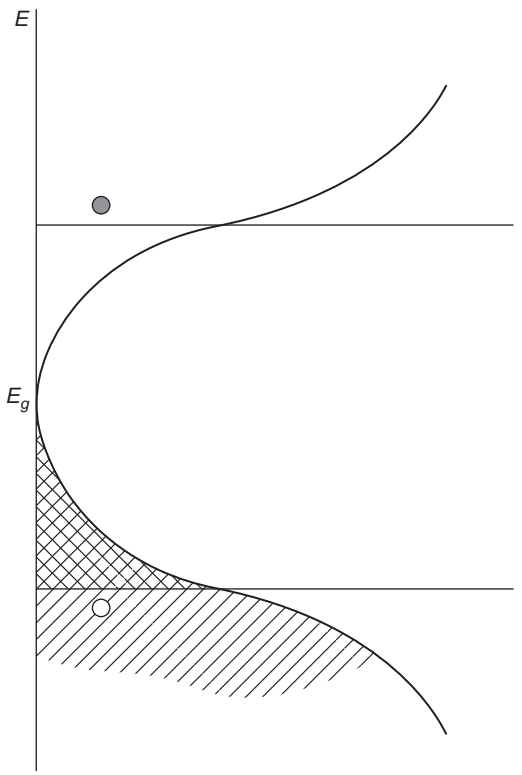

FIGURE 9.11
The nonconducting tail states in a distorted tetrahedral semiconductor arise from the distorted bonds.

In addition, an amorphous tetrahedral semiconductor has imperfectly coordinated atoms, and thereby, the bonds are uncompensated. These are known as "dangling" bonds, each of which has limited degeneracy. A dangling bond has an empty state and an electron associated with it. Because these bonds are uncompensated, both the electron and the empty state are localized at 0° K. Thus, the immobile states are separate but overlapping, and the distributions are obtained within the energy gap. In fact, the concentration of the dangling bonds is on the order of 10^{25} m^{-3}. Due to this unusually high concentration of the dangling bonds, each of which produces a localized electron and a localized empty state, the Fermi level (μ) is at the center of the energy gap. Thus, the amorphous semiconductors essentially become insensitive to doping. The "band" picture of an amorphous tetrahedral semiconductor is shown in Figure 9.12.

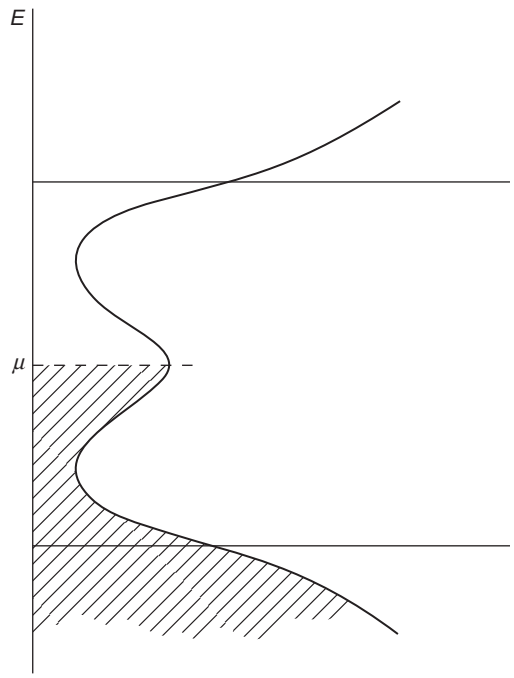

FIGURE 9.12

The band picture of amorphous tetrahedral semiconductors including tail states.

PROBLEMS

9.1. The effective mass of electrons and holes in a semiconductor can be expressed as

$$[\mathbf{M}_n^{-1}(\mathbf{k})]_{ij} = \pm \frac{1}{\hbar^2} \frac{\partial^2 \varepsilon_n}{\partial k_i \partial k_j}, \tag{1}$$

where the positive sign is for electrons and the negative sign is for holes. Because the bottom of the conduction band is at ε_c and the top of the valence band is at ε_v, show that the energy of the electrons $(\varepsilon_e(\mathbf{k}))$ and holes $(\varepsilon_h(\mathbf{k}))$ can be written as

$$\varepsilon_e(\mathbf{k}) = \varepsilon_c + \frac{\hbar^2}{2} \sum_{ij} k_i (\mathbf{M}_e^{-1})_{ij} k_j \tag{2}$$

and

$$\varepsilon_h(\mathbf{k}) = \varepsilon_v - \frac{\hbar^2}{2} \sum_{ij} k_i (\mathbf{M}_h^{-1})_{ij} k_j. \tag{3}$$

9.2. Show that the density of states in the conduction and valence bands can be expressed as

$$\begin{aligned} g_c(\varepsilon) &= \frac{\sqrt{2m_n^{*3}\varepsilon'}}{\pi^2\hbar^3}\eta_c, \quad \varepsilon > \varepsilon_c \\ &= 0, \qquad\qquad\quad \varepsilon \leq \varepsilon_c, \end{aligned} \tag{1}$$

where

$$\varepsilon' \equiv \varepsilon - \varepsilon_c \tag{2}$$

and

$$\begin{aligned} g_v(\varepsilon) &= \frac{\sqrt{2m_p^{*3/2}|\varepsilon''|}}{\pi^2\hbar^3}, \quad |\varepsilon''| > \varepsilon_v \\ &= 0, \qquad\qquad\quad |\varepsilon''| \le \varepsilon_v, \end{aligned} \tag{3}$$

where

$$|\varepsilon''| \equiv |\varepsilon - \varepsilon_v|. \tag{4}$$

Here, η_c is the number of symmetrically equivalent minima in the conduction band (six for Si and eight for Ge). m_n^* and m_p^* are the density of states' effective mass of electrons and holes that are obtained from the relation

$$m_n^* = \left(m_1^e m_2^e m_3^e\right)^{1/2} \tag{5}$$

and

$$m_p^{*3/2} = \left(m_{pl}^*\right)^{3/2} + \left(m_{ph}^*\right)^{3/2}, \tag{6}$$

where

$$m_{pl}^* = \left(m_1^{lh} m_2^{lh} m_3^{lh}\right)^{1/2} \tag{7}$$

and

$$m_{ph}^* = \left(m_1^{hh} m_2^{hh} m_3^{hh}\right)^{1/2}. \tag{8}$$

Here, m_{pl}^* and m_{ph}^* are the effective masses of the light and heavy holes.

9.3. From Eq. (9.32) and in analogy with the free electron model, one can write the conductivity σ_i of an intrinsic semiconductor as

$$\sigma_i = \frac{n_i e^2 \tau_e}{m_n^*} + \frac{p_i e^2 \tau_h}{m_p^*}, \tag{1}$$

where τ_e and τ_h are the relaxation times for electrons and holes. Show that Eq. (9.48) can be written in the alternate and more familiar form

$$\sigma_i = n_i e \mu_e + p_i e \mu_h, \tag{2}$$

where μ_e and μ_h are the mobility of the electrons and holes, which is the velocity (always defined as positive) of the carriers in a unit electric field.

9.4. We have derived an expression for the valence band

$$p_v(T) = \frac{\sqrt{2m_p^{*3}}}{\pi^2\hbar^3} e^{(\varepsilon_v - \mu)/k_B T} \int_0^\infty |\varepsilon''|^{1/2} e^{-|\varepsilon''|/k_B T} d|\varepsilon''|. \tag{1}$$

It can be easily shown that

$$\int_0^\infty \varepsilon^{1/2} e^{-\varepsilon/k_B T} d\varepsilon = \frac{1}{2}(k_B T)^{3/2}\pi^{1/2}. \tag{2}$$

From Eqs. (1) and (2), show that

$$p_v(T) = \wp_v(T) e^{(\varepsilon_v - \mu)/k_B T}, \tag{3}$$

where

$$\wp_v(T) = 2\left(\frac{m_p^* k_B T}{2\pi\hbar^2}\right)^{3/2}. \tag{4}$$

$\wp_v(T)$ can be expressed numerically as

$$\wp_v(T) = 2.51\left(\frac{m_p^*}{m}\right)^{3/2}\left(\frac{T}{300\ \text{K}}\right)^{3/2} 10^{19}\ \text{cm}^{-3}. \tag{5}$$

9.5. Substitute the expressions for Ω_1 and Ω_2 derived in Eqs. (9.105) and (9.106) in Eq. (9.84) and neglect the complex spin-orbit terms. Show that the expression for the spin contribution to the EPR shift at the jth site is

$$P_{js}^{\nu\mu} = -\frac{1}{2}\sum_{n\vec{k}\rho\rho'}\left(\frac{1}{2g_j}\sigma^\nu \mathfrak{F}\right)_{n\rho,n\rho'} g_{nn}^\mu(\vec{k})\sigma_{n\rho',n\rho}^\mu f'(E_{n\vec{k}}), \tag{1}$$

where the effective g factor $g_{nn}^\mu(\vec{k})$ is defined as

$$g_{nn}^\mu(\vec{k})\sigma_{n\rho',n\rho}^\mu = g_0\sigma_{n\rho',n\rho}^\mu + \frac{2i}{m}\in_{\alpha\beta\mu}\sum_{m\neq n,\rho''}\frac{\pi_{n\rho',m\rho''}^\alpha \pi_{m\rho'',n\rho}^\beta}{E_{mn}}. \tag{2}$$

9.6. If the Bloch-type tight-binding sums for valence-band basis functions are constructed by taking a linear combination of the hybrids forming a bond

$$\chi_j^v(\mathbf{r},\mathbf{k}) = \sum_i f_j^v(\mathbf{k}) e^{i\mathbf{k}\cdot\mathbf{R}_i}[h_j^1(\mathbf{r}-\mathbf{R}_i) + \lambda h_j^2(\mathbf{r}-\mathbf{R}_i-\mathbf{d}_j)e^{i\mathbf{k}\cdot\mathbf{d}_j}], \tag{1}$$

where

$$f_j^v(\mathbf{k}) = [N(1+\lambda^2+2\lambda S\cos\ \mathbf{k}\cdot\mathbf{d}_j)]^{-1/2}, \tag{2}$$

show that the basis functions for the conduction band $\chi_j^c(\mathbf{r},\mathbf{k})$ are obtained by constructing functions orthogonal to $\chi_j^v(\mathbf{r},\mathbf{k})$:

$$\chi_j^c(\mathbf{r},\mathbf{k}) = \sum_i f_j^c(\mathbf{k}) e^{i\mathbf{k}\cdot\mathbf{R}_i}[(\lambda + Se^{i\mathbf{k}\cdot\mathbf{d}_j})h_j^1(\mathbf{r}-\mathbf{R}_i) - (\lambda S + e^{i\mathbf{k}\cdot\mathbf{d}_j})h_j^2(\mathbf{r}-\mathbf{R}_i-\mathbf{d}_j)], \tag{3}$$

where

$$f_j^c(\mathbf{k}) = \left[\frac{\lambda + Se^{-i\mathbf{k}\cdot\mathbf{d}_j}}{N(1-S^2)(1+\lambda^2+2\lambda S\cos\ \mathbf{k}\cdot\mathbf{d}_j)(\lambda + Se^{i\mathbf{k}\cdot\mathbf{d}_j})}\right]^{1/2}. \tag{4}$$

9.7. Show that the Bloch eigenfunctions for the valence and conduction bands

$$\psi_n(\mathbf{r},\mathbf{k}) = \sum_j \alpha^v_{jn}(\mathbf{k})\chi^v_j(\mathbf{r},\mathbf{k}) \tag{1}$$

and

$$\psi_m(\mathbf{r},\mathbf{k}) = \sum_j \alpha^c_{jm}(\mathbf{k})\chi^c_j(\mathbf{r},\mathbf{k}) \tag{2}$$

are orthonormal. Here, α's are elements of (4×4) unitary matrices

$$\sum_n \alpha^v_{jn}(\mathbf{k})\alpha^{v\dagger}_{nj'}(\mathbf{k}) = \delta_{jj'} \tag{3}$$

and

$$\sum_m \alpha^c_{jm}(\mathbf{k})\alpha^{c\dagger}_{mj'}(\mathbf{k}) = \delta_{jj'}. \tag{4}$$

References

1. Ashcroft NW, Mermin ND. *Solid state physics*. New York: Brooks/Cole; 1976.
2. Chadi DJ, White RM, Harrison WA. Theory of the magnetic susceptibility of tetrahedral semiconductors. *Phys Rev Lett* 1975;**35**:1372.
3. Coulson CA, Redei LB, Stocker D. The electronic properties of tetrahedral intermetallic compounds I. charge distribution. *Proc R Soc* 1962;**270**:357.
4. Das RK, Tripathi GS, Misra PK. Theory of the spin EPR shift: application to Pb1-xMnxTe. *Phys Rev B* 2005;**72**:035216.
5. Eggenkamp PJT, Swegten HJM, Story T, Litvinov VI, Swuste CHW, de Jonge WJM. Calculations of the ferromagnet-to-spin-glass transition in diluted magnetic systems with RKKY interaction. *Phys Rev* 1995; **51**:15250.
6. Furdyna JK, Kossut J, eds. *Diluted magnetic semiconductors.* Boston: Academic Press; 1988.
7. Kittel C. *Introduction to solid state physics*. New York: John Wiley & Sons; 1976.
8. Louie SG. Quasiparticle excitations and photoemission. *Stud Surf Sci Catal* 1992;**74**:32.
9. Luttinger JM, Kohn W. Motion of electrons and holes in perturbed periodic fields. *Phys Rev* 1969;**97**:869.
10. Marder MP. *Condensed matter physics*. New York: John Wiley & Sons; 2000.
11. Misra SK, Misra PK, Mahanti SD. Many-body theory of magnetic susceptibility of electrons in solids. *Phys Rev B* 1982;**26**:1903.
12. Nucho RN, Ramos JG, Wolff PA. Chemical-bond approach to the magnetic susceptibility of semiconductors. *Phys Rev B* 1978;**17**:1843.
13. Polk DE. Structural model for amorphous silicon and germanium. *J Non-Cryst Solids* 1971;**5**:365.
14. Sahu T, Misra PK. Magnetic susceptibility of tetrahedrally coordinated solids. *Phys Rev B* 1982;**26**:6795.
15. Sukhatme VP, Wolff PA. Chemical-bond approach to the magnetic susceptibility of tetrahedral semiconductors. *Phys Rev Lett* 1975;**35**:1369.
16. Trellakis A. Nonperturbative solution for Bloch electrons in constant magnetic fields. *Phys Rev Lett* 2003;**91**:056405.
17. Tripathi GS, Das LK, Misra PK, Mahanti SD. Theory of spin-orbit and many-body effects of the Knight shift. *Phys Rev B* 1982;**25**:3091.
18. Vennix CWHM, Frikkee E, Eggenkamp PJT, Swagten HJM, Kopinga K, de Jonge WJM. Neutron-diffraction study of the carrier-concentration-induced ferromagnet-to-spin-glass transition in the diluted magnetic semiconductor Sn1-xMnxTe. *Phys Rev B* 1993;**48**:3770.